Density Functional Theory Calculations of Vibrational Absorption and Circular Dichroism Spectra of Dimethyl-L-tartrate

Thierry Buffeteau,*,† Laurent Ducasse,† Aurélie Brizard,‡ Ivan Huc,‡ and Reiko Oda‡

Laboratoire de Physico-Chimie Moléculaire, UMR 5803 du CNRS, Université Bordeaux I, 351 Cours de la Libération, 33405 Talence, France, and Institut Européen de Chimie et Biologie, 16 Av. Pey Berland, 33607 Pessac, France

Vibrational absorption and circular dichroism (VCD) spectra of dimethyl-L-tartrate have been measured in CCl$_4$ solution in the mid-infrared spectral range. Experimental spectra have been compared with the density functional theory (DFT) absorption and VCD spectra calculated using the B3LYP functional and 6-31G* basis set for nine conformers of dimethyl-L-tartrate. The minimum-energy structure of each conformer has been calculated without constraining the molecule to be of C_2 symmetry. These calculations indicate that the trans COOR conformation with hydrogen bonding between the OH and C=O groups attached to the same chiral carbon is of lowest energy and represents more than 83% of the different conformers at room temperature. The vibrational absorption and circular dichroism calculated from this conformation are in very good overall agreement with experiment. Finally, the limitation of the coupled oscillator model has been shown to interpret the VCD response in the OH stretching region.

1. Introduction

Vibrational circular dichroism (VCD) is a chiral molecule's differential absorption of left- and right-handed circularly polarized radiation in the infrared region.[1] The VCD spectrum of a chiral molecule is very dependent on its absolute configuration and, in the case of flexible molecules, on its conformation. The relation between the VCD spectrum and the structure of a chiral molecule can be rationalized from theoretical calculations.[2] By comparing the experimental spectrum with the calculated spectrum of one enantiomer with a given conformation, it is possible to identify the absolute configuration and the conformation of a chiral molecule. This application of VCD has been used extensively in past years for two main reasons: (i) VCD spectra of chiral molecules in solution can be easily measured over a large spectral range ($\bar{v} > 700$ cm^{-1}) with a good signal-to-noise ratio at acceptable resolution (4 cm^{-1}) using a commercial FTIR spectrometer; (ii) reliable predictions of VCD spectra of chiral molecules over a wide range of molecular size can be performed using density functional theory (DFT).

Since Holzwarth and Chabay predicted observable rotational strengths for vibrational bands of chiral dimers,[3] dimethyl tartrate [−C*H(OH)−COOCH$_3$]$_2$ has been a good candidate for vibrational circular dichroism studies. Moreover, they developed the degenerate coupled oscillator (DCO) model to explain the VCD spectra of this type of chiral molecule. This model can be applied to VCD by analogy to the exciton coupling theory of electronic circular dichroism.[4] Accordingly, the determination of the conformation of dimethyl tartrate in solution was one of the first applications of VCD to stereochemical analysis, but it was a controversial problem. Keiderling and co-workers carried out VCD measurements in the OH and C=O stretching regions[5−7] and used the DCO model to interpret the bisignate VCD observed in these two regions. They assumed that the rotational

strengths measured on this dimerlike molecule are not due to the intrinsic chirality of the oscillators but result only from their coupling. The VCD signal thus presents a positive and a negative lobe of the same intensity with a Lorentzian derivative shape whose intensity and sign depend on the relative angle between the oscillators and consequently on the geometry of the molecule. Calculations for a trans hydroxyl group conformation reproduced the experimental signs in the two regions.[6] Two different possibilities were suggested for internal hydrogen bonding: one with hydrogen bonding between OH and OCH$_3$ groups from opposite halves of the molecule and another with hydrogen bonding between OH and C=O groups attached to the same chiral carbon. This last possibility has been considered by Freedman and co-workers to interpret the single VCD band observed in the CH stretching region, using the ring-current model.[8] In this last work, the choice between the trans OH and trans COOR conformations seems to be unimportant. More recently, ab initio (Hartree−Fock) geometry calculations on tartaric acid by Polavarapu and co-workers indicated that the most stable conformation corresponds to trans COOR groups, with hydrogen bonding between OH and C=O groups attached to the same chiral carbon.[9] Because the VCD associated with the C*−O stretching vibration was identical in tartaric acid and in its esters, a trans COOR conformation was suggested for dimethyl tartrate.

In this paper, we present DFT calculations of absorption and VCD spectra of dimethyl-L-tartrate to determine the most favorable conformations of this chiral molecule in the gas phase and in solution. Nine conformers of dimethyl-L-tartrate were investigated. Then, the optimized geometry of the most stable conformer was used to demonstrate the limitations of the coupled oscillator model in the interpretation of VCD in the OH stretching region.

2. Experimental Section

Materials. (+)-(2R,3R)-Dimethyl tartrate (named dimethyl-L-tartrate in this paper) was obtained from Aldrich and was studied without further purification as dilute solutions in CCl$_4$.

* To whom correspondence should be addressed: E-mail: t.buffeteau@lpcm.u-bordeaux1.fr. Fax: (33) 5 40 00 84 02.
† Université Bordeaux I.
‡ Institut Européen de Chimie et Biologie.
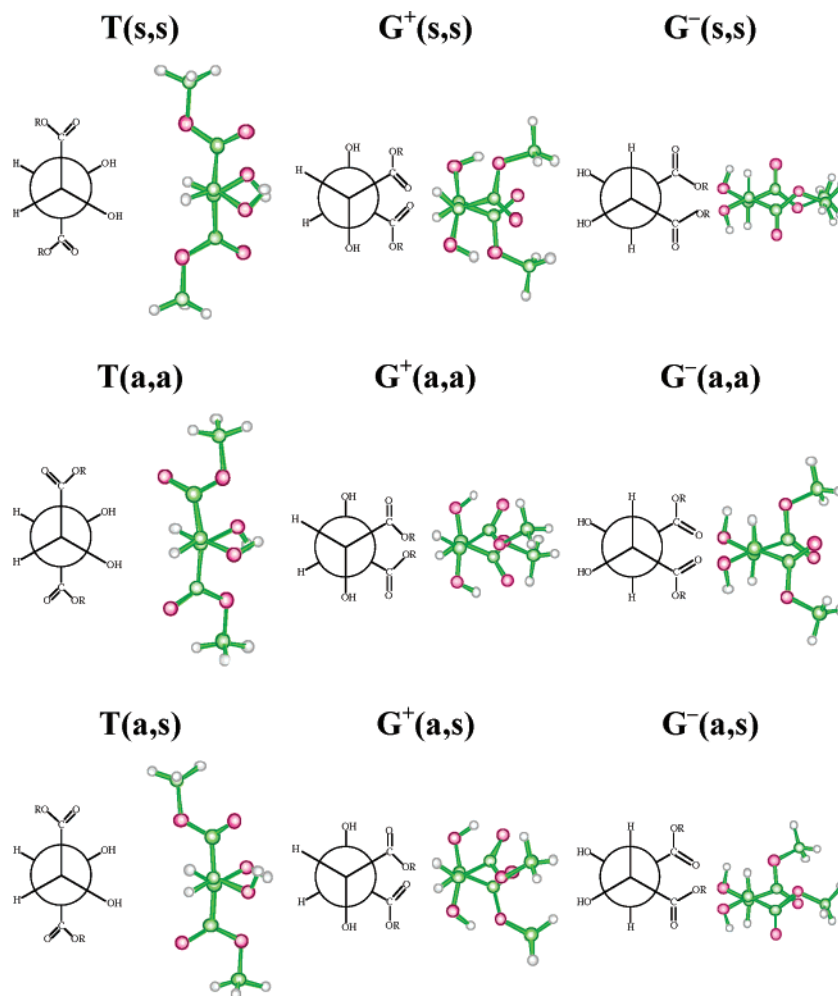
Figure 1. Different conformers of dimethyl-L-tartrate. The COOR trans conformers are in the first (Newman projection) and second (optimized geometry) columns, the OH trans conformers are in the third (Newman projection) and fourth (optimized geometry) columns, and the H trans conformers are in the fifth (Newman projection) and sixth (optimized geometry) columns. The C−OH/C=O synplanar conformers are on the first row, the C−OH/C=O antiplanar conformers are on the second row, and the mixed eclipsed conformers are on the third row.

FTIR Measurements. The infrared and VCD spectra were recorded on a Nicolet Nexus 670 FTIR spectrometer equipped with a VCD optical bench. In this optical bench, the light beam is focused by a ZnSe lens ($f = 190$ mm) onto the sample, passing an optical filter (depending on the studied spectral range), a BaF_2 wire grid polarizer (Specac), and a ZnSe photoelastic modulator (Hinds Instruments). The light is then focused by a ZnSe lens ($f = 40$ mm) onto a 1×1 mm^2 HgCdTe detector. The VCD spectra were recorded for 8 h data collection time at 8- and 4-cm^{-1} resolution in the OH/CH (3700−2750 cm^{-1}) and C=O/C−O (1800−1000 cm^{-1}) stretching regions, respectively. Spectra were measured in CCl_4 solvent at a concentration of 0.025 M (0.010 M) and at a path length of 1.5 mm (0.5 mm) for the OH/CH (C=O/C−O) stretching regions. In the presented absorption spectrum, the solvent absorption was subtracted out.

Calculations. The geometries and vibrational frequencies of different conformers of dimethyl-L-tartrate were calculated by means of quantum chemical approaches. The geometries were fully optimized by using density functional theory (DFT) with the nonlocal functional B3LYP[10] and the 6-31G* basis set.[11] The calculations were performed in the gas and solvated phases. For systems in nonaqueous solutions, self-consistent reaction field (SCRF) methods are commonly used; in these methods, the solvent is modeled as a continuum of the uniform dielectric constant ϵ (the reaction field). The solute is placed into a cavity within the solvent. SCRF approaches differ in how they define

the cavity and the reaction field. The simplest SCRF model is the Onsager model in which the solute occupies a fixed spherical cavity of radius a_0 within the solvent field.[12] Gaussian code can produce an estimated value of a_0. The absorption and VCD spectra were calculated in the gas phase at the same level of theory. All calculations were performed with the Gaussian 98 package.[13] The theoretical absorption and VCD spectra were simulated with Lorentzian band shapes and 15- and 5-cm^{-1} half-width at half-height values in the OH/CH and C=O/C−O stretching regions, respectively. Because the calculated band positions are higher than the experimental values, the frequencies were scaled with a frequency-independent factor of 0.97.

3. Results and Discussion

Three principal conformations differing in the dihedral angle C−C*−C*−C (labeled T, G$^+$, and G$^-$ for trans COOR, trans OH, and trans H conformers, respectively) and two principal COH/C=O rotamers around the C−C* bond (labeled s and a for synplanar and antiplanar orientations, respectively) are considered. Because the rotamers of the two halves of the molecule can be identical ((s, s) or (a, a)) or mixed (a, s) for each principal conformation, nine possible conformations of dimethyl-L-tartrate are investigated (Figure 1). The minimum-energy structure of each conformer has been calculated without constraining the molecule to be of C_2 symmetry and the OCC*O

TABLE 1: Conformations and Energies of Dimethyl-L-tartrate

conformer	dihedral angle (°)		intramolecular hydrogen bonding	energy (hartrees)	ΔE^a (kJ/mol)	pop %
	C–C*–C*–C	H–O–C*–C				
T(s, s)	173.7	−15.8 , −15.8	*(structure)*	−685.995246	0	70.2
T(a, a)	−164.6	−67.6 , 18.3	bifide [b] *(structure)*	−685.988838	16.79	0.1
T(a, s)	−170.7	−66.7 , 6.4	bifide [b] *(structure)*	−685.993572	4.38	11.6
G⁺(s, s)	44.6	−25.5 , −25.5	*(structure)*	−685.992119	8.18	2.5
G⁺(a, a)	62.3	−66.7 , −66.7	*(structure)*	−685.993837	3.67	15.5
G⁺(a, s)	56.7	−62.3 , −69.0	*(structure)*	−685.989259	15.68	0.1
G⁻(s, s)	−56.4	−29.6 , −29.6	*(structure)*	−685.982640	19.25	0.
G⁻(a, a)	−47.4	−47.4 , −47.4	*(structure)*	−685.987905	33.05	0.
G⁻(a, s)	−53.6	−28.8 , −47.3	*(structure)*	−685.985740	24.92	0.
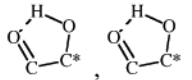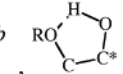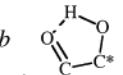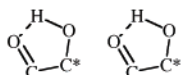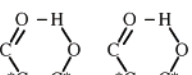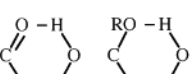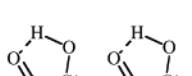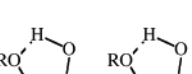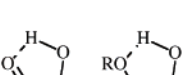
[a] Energy difference relative to the lowest-energy conformer. [b] In the bifide structure of the hydrogen bonding, the oxygen of the opposite hydroxyl group and the oxygen of the OR group of the same half of the molecule take part in the hydrogen bonding.
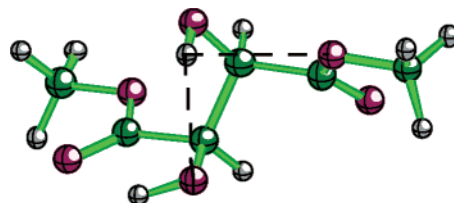
groups to be planar. However, as shown in Figure 1, every (s, s) and (a, a) conformer exhibits a C_2 symmetry axis after optimization. Table 1 lists the converged C–C*–C*–C and H–O–C*–C dihedral angles, the type of intramolecular hydrogen bonding for the two halves of the molecule, the optimized energies, and the relative population at 273 K based on the electronic energies for each conformer. It clearly appears that the trans COOR conformation with hydrogen bonding between the OH and C=O groups attached to the same chiral carbon is of lowest energy and represents more than 70% of the different conformers at room temperature. This result is in agreement with the ab initio geometry calculations on tartaric acid of Polavarapu and co-workers.[9] Three other conformers present non-negligible populations in the gas phase (G⁺(a, a) > T(a, s) > G⁺(s, s)) whereas the relative populations of the remaining conformers are small enough to have no significant impact on the calculated vibrational properties.

The B3LYP/6-31G* absorption and VCD spectra of the four most stable conformers are reported in Figures 2 and 3 and compared to the experimental spectra. The predicted absorption spectrum of the T(s, s) conformer is in good agreement with the experimental spectrum, except in the CH stretching region.

DFT-Calculated Dimethyl-L-tartrate Spectra

J. Phys. Chem. A, Vol. 108, No. 18, 2004 **4083**
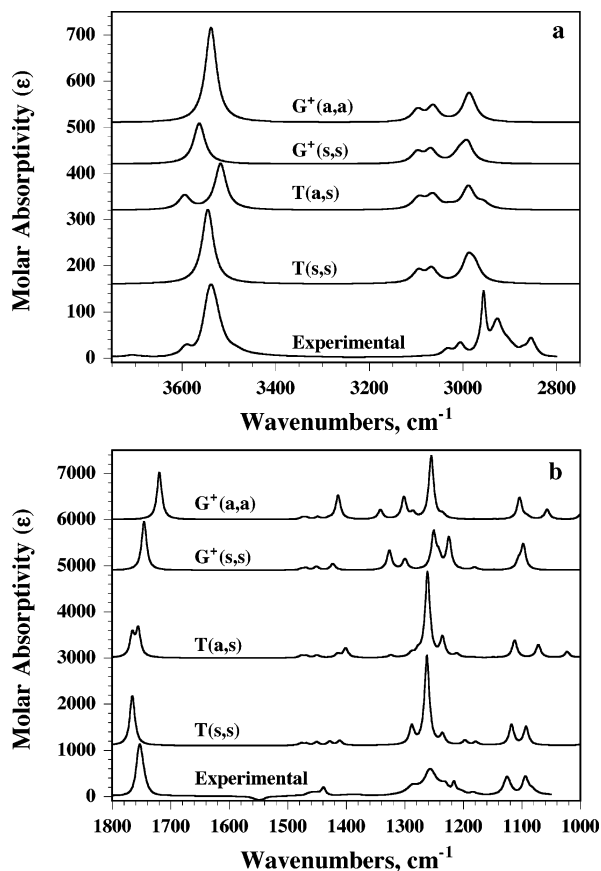
Figure 2. Comparison of the experimental absorption spectrum of dimethyl-L-tartrate in CCl₄ solution with the DFT absorption spectra of the four most stable conformers calculated using the B3LYP/6-31G* basis set in (a) the 3750−2750-cm⁻¹ and (b) the 1800−1000-cm⁻¹ regions. The theoretical spectra were simulated with Lorentzian band shapes and 15- and 5-cm⁻¹ half-widths in the 3750−2750-cm⁻¹ and 1800−1000-cm⁻¹ regions, respectively. The frequencies were scaled by 0.97.

Figure 3. Comparison of the experimental VCD spectrum of dimethyl-L-tartrate in CCl₄ solution with the DFT VCD spectra of the four most stable conformers calculated using the B3LYP/6-31G* basis set in (a) the 3750−2750-cm⁻¹ and (b) the 1800−1000-cm⁻¹ regions. The theoretical spectra were simulated with Lorentzian band shapes and 15- and 5-cm⁻¹ half-widths in the 3750−2750-cm⁻¹ and 1800−1000-cm⁻¹ regions, respectively. The frequencies were scaled by 0.97.

The calculated frequencies (scaled by 0.97) and the vibrational assignments based on a normal coordinate analysis are reported in Table 2 for the most important bands of the T(s, s) conformer. Because of the C_2 symmetry of this dimerlike molecule, the normal modes of vibrations are classified into two symmetry species A and B (in-phase and out-of-phase around the C_2 axis, respectively), both modes being active in the infrared spectra. Most of the vibrations (not reported in Table 2) present a small splitting in frequency (lower than 2 cm⁻¹), indicating a small coupling of the associated oscillators, except for the methine stretching mode ($\Delta \nu = 10$ cm⁻¹) and the C−O stretching modes of the C*−OH and C−O−CH₃ groups ($\Delta \nu \approx 25$ cm⁻¹). If the value of the splitting is lower than the width of the band, then only one band is observed in the absorption spectrum. As shown in Figure 2a and considering the intramolecular hydrogen bonding obtained for the four most stable conformers, we find that the strong band at 3538 cm⁻¹ is characteristic of the OH stretching vibration in the OH- - -O=C hydrogen-bonded conformer whereas the shoulder observed at 3589 cm⁻¹ indicates that the T(a, s) conformer is present in solution and that the bifide structure of hydrogen bonding occurs. In the CH stretching region, the simulated absorption spectra differ from the experimental spectrum: (i) the calculated frequencies are systematically higher than the experimental ones, and (ii) the number of bands and their intensities are not reproduced. Indeed, two bands are observed at 2956 and 2855 cm⁻¹ in the experimental spectrum whereas only one is calculated at 2989.8

cm⁻¹. This discrepancy arise from the strong Fermi resonance between the symmetric methyl stretching fundamental and the overtone of the antisymmetric methyl deformation, which cannot be reproduced at this level of calculation. Moreover, the frequencies calculated by DFT that are too high arise from the anharmonicity of the CH stretching modes. A lower frequency-independent factor (0.95 instead 0.97) should be applied if one is interested in a better matching.

As previously published, the experimental VCD spectrum of dimethyl-L-tartrate shows a Lorentzian derivative shape for the OH, C=O, and C−O stretching vibrations. These VCD couplets arise from the coupling of a pair of oriented dipoles for each vibration (in- and out-of-phase modes) and were interpreted using the degenerate coupled oscillator (DCO) model.[3] The coupling of large dipoles can lead to intense VCD couplets as observed in Figure 3b for the C=O and C−O stretching vibrations. However, because of the opposite sign of the two components, there is a significant cancellation of the VCD couplets for broad band and/or small coupling (small splitting). This feature can explain the small intensity of the VCD couplet in the OH stretching region. In contrast to the VCD couplets observed in the OH, C=O, and C−O stretching regions, the experimental VCD spectrum reveals a single band in the CH stretching region. The nonobservation of a bisignate VCD has been explained by the low value of the dipolar strength of the methine vibration and consequently the low intensity of the rotational strength due to coupling. Moreover, Freedman and

TABLE 2: Calculated Frequencies, Dipolar and Rotational Strengths, and Assignments of Some Bands of the T(s, s) Conformer of Dimethyl-L-tartrate

mode	frequencies cm^{-1}	D 10^{-40} esu^2 cm^2	R 10^{-44} esu^2 cm^2	symmetry[a]	assignments[b]
29	1092.9	509.1	−175.7	B	ν C*O (0.66) δ C*OH (0.09) ν CO (0.07) δ C*C*O (0.05)
30	1117.6	553.6	367.6	A	ν C*O (0.53) ν C*C* (0.14) δ C*OH (0.12)
37	1262.2	2150.9	−416.4	B	ν CO (0.43) δ C*OH (0.15) ν CC (0.14) δ CC*H (0.07) δ C*C=O (0.05) δ OC=O (0.05)
38	1288	387.7	451.6	A	δ C*OH (0.25) ν CO (0.22) ν CC (0.11) ν C*O (0.10) δ HC*O (0.09) δ CC*H (0.06) δ C*C=O (0.05)
49	1764	272.7	−310.1	B	ν C=O (0.83) ν CO (0.07)
50	1766.3	619.3	277.6	A	ν C=O (0.83) ν CO (0.07)
51	2965.8	3.7	9.7	B	ν C*H (0.99)
52	2975.4	42.3	−40.7	A	ν C*H (0.99)
59	3544.7	147.0	193.7	B	ν OH (1.00)
60	3546.4	44.4	−190.9	A	ν OH (1.00)

[a] A and B symmetries correspond to in-phase and out-of-phase modes, respectively. [b] Contributions to a potential energy distribution larger than 0.05.

co-workers have proposed that the vibration of each methine can generate a ring current around the adjacent five-membered

ring, which would result in an enhanced contribution to the rotational strength.[8]

The experimental VCD spectrum of dimethyl-L-tartrate is fairly well reproduced by the predicted spectrum of the T(s, s) conformer, indicating that the dilute CCl$_4$ solution contains mainly this conformer. In contrast, the predicted VCD spectra of the other conformers present important differences with experimental data. The populations calculated from the electronic energies of the optimized geometries are apparently overestimated. The contribution of the G$^+$(a, a) conformer, associated with a room-temperature population of 15.5%, which presents a VCD spectrum very different from the experimental one, seems to be especially too large. A more reliable estimate of the conformer population can be calculated using Gibbs energies. Indeed, Gibbs energies include thermal effects in the calculation of the energetic values and the whole set of vibrational degrees of freedom. The comparison of the conformer population calculated from the electronic and Gibbs energies is reported in Table 3. The main difference between the populations derived from electronic energies versus Gibbs energies concerns the G$^+$(a, a) conformer whose population drops from 15.5 to 3.1%. Finally, to determine more precisely the contribution of the different conformers in CCl$_4$ solution, the effect of solvation on the optimized geometries was introduced phenomenologically through a continuum model calculation. The electronic energies and relative populations calculated from the Onsager model and by considering the

TABLE 3: Relative Populations Based on Electronic and Gibbs Energies in Gas and Solvated Phases

	gas phase				solvated phase	
	electronic energies		Gibbs energies		electronic energies	
conformer	ΔE[a] (kJ/mol)	population %	ΔE[a] (kJ/mol)	population %	ΔE[a] (kJ/mol)	population %
T(s, s)	0[b]	70.2	0[c]	83.5	0[d]	88.6
T(a, a)	16.79	0.1	15.17	0.2		
T(a, s)	4.38	11.6	5.15	10.1	5.60	8.9
G$^+$(s, s)	8.18	2.5	8.07	3.0	8.67	2.5
G$^+$(a, a)	3.67	15.5	8.03	3.1	8.83	0.[e]
G$^+$(a, s)	15.68	0.1	17.83	0.1		
G$^-$(s, s)	19.25	0.	19.98	0.		
G$^-$(a, a)	33.05	0.	29.70	0.		
G$^-$(a, s)	24.92	0.	23.97	0.		

[a] Energy difference relative to the lowest-energy conformer. [b] The electronic energy of this conformer is −685.995246 hartrees. [c] The Gibbs energy of this conformer is −685.864660 hartrees. [d] The electronic energy of this conformer is −685.995777 hartrees. [e] See the discussion in the text for the G$^+$(a, a) conformer.

dielectric constant of CCl$_4$ (2.203) are reported in Table 3 for the four most stable conformers. The relative population of the T(s, s) conformer increases with regard to the gas-phase results (88.6%). The contribution of the T(a, s) conformer is still significant (8.9%) whereas the contribution of the G$^+$(s, s) conformer is not affected (~2.5%). In contrast, the situation of the G$^+$(a, a) conformer is less evident. Starting from the optimized geometry of the G$^+$(a, a) conformer in the gas phase, the optimization procedure using the Onsager model leads to the solvated optimum geometry of the G$^+$(s, s) conformer. This point reveals that the very compact shape of the G$^+$(a, a) conformer should not be stabilized in the presence of a solvent and that this conformer does not exist in solution and does not contribute to the VCD spectrum of dimethyl-L-tartrate.

DFT-Calculated Dimethyl-L-tartrate Spectra

J. Phys. Chem. A, Vol. 108, No. 18, 2004 **4085**

As mentioned above, the VCD spectrum of dimethyl-L-tartrate can be interpreted using the degenerate coupled-oscillator (DCO) model. If the intrinsic chirality of each oscillator is omitted (i.e., the magnetic dipole transition moment for each oscillator is zero), then the DCO equation for the rotational strength is given by[3]

$$\mathrm{R}^{\pm} = \mp \left(\frac{\pi}{2}\nu_0\right)\vec{R}_{12}\cdot(\vec{\mu}_1 \times \vec{\mu}_2) \quad (1)$$

where $\vec{\mu}_1$ and $\vec{\mu}_2$ are the transition dipole moments, $\vec{R}_{12}$ is the vector from $\vec{\mu}_1$ to $\vec{\mu}_2$, and ν_0 is the wavenumber of the transition. The upper signs give the rotational strength R^+ of the symmetric combination of stretches (in-phase mode). The splitting of the in-phase (+) and out-of-phase (−) modes can be calculated by the dipolar coupling equation[4]

$$V_{12} = \frac{1}{|\vec{R}_{12}|^3}\left(\vec{\mu}_1\cdot\vec{\mu}_2 - \frac{3(\vec{R}_{12}\cdot\vec{\mu}_1)(\vec{R}_{12}\cdot\vec{\mu}_2)}{|\vec{R}_{12}|^2}\right) \quad (2)$$

and

$$\nu^{\pm} = \nu_0 \pm V_{12} \quad (3)$$

Assuming that the two dipoles are equivalent ($\vec{\mu}_1 = \vec{\mu}_2 = \vec{\mu}$) and using the angular conventions provided in Tinoco's paper ($\vec{\mu}_1$ in the xy plane and $\vec{R}_{12}$ along the $\vec{x}$ axis),[4] we can rewrite relations 1 and 2 ($\theta_1 = 90°$):

$$\mathrm{R}^{\pm} = \mp\left(\frac{\pi}{2}\nu_0\right)\mu^2 R_{12}\sin\phi_1\cos\theta_2 \quad (4)$$

$$V_{12} = \frac{\mu^2}{R_{12}^3}(\sin\theta_2\cos(\phi_1 - \phi_2) - 3\sin\theta_2\cos\phi_1\cos\phi_2) \quad (5)$$

where ϕ_1, θ_1, ϕ_2, and θ_2 are the azimuthal and tilt angles of dipoles 1 and 2, respectively.

The magnitude of μ can be obtained from the experimental molar absorptivity spectrum $\epsilon(\nu)$ of the band by calculating the dipolar strength, D, with the relation $\mu = (^D/_2)^{1/2}$ where $D = 0.92 \times 10^{-38}\int \epsilon(\nu)/\nu \, d\nu$.

We have calculated the DCO effects expected in the OH and C=O bands for the T(s, s) conformer. The orientation angles ϕ_1, ϕ_2, and θ_2 can be easily determined from the Cartesian coordinates (Z matrix) of the optimized geometry of the T(s, s) conformer. Under these conditions, we assume that the directions of the transition dipole moments are along the chemical bonds. The orientation angles of the OH and C=O dipoles and the DCO and DFT results of splitting and rotational strength are listed in Table 4. The DCO model reproduces the observed VCD sign pattern for the C=O mode but the opposite sign pattern for the OH mode. In this last case, the sign of the rotational strength is in agreement with the DFT calculations but not with the sign of the splitting V_{12}. It is noteworthy that the value of θ_2 is close to zero. Because V_{12} is proportional to $\sin\theta_2$, a small variation in θ_2 can change the sign of the splitting. A possible variation of θ_2 can come from the determination of the directions of the transition dipole moments. These directions were determined more precisely from the DFT dipole derivative components. The new orientation angles of the OH and C=O dipoles and the corresponding splitting and rotational strengths are also listed in Table 4. The agreement between the DCO model and the DFT calculation is better for the C=O mode, but the opposite sign of the splitting is still calculated for the

TABLE 4: Orientation Angles and DCO and DFT Splitting and Rotational Strengths of the T(s, s) Conformer of Dimethyl-L-tartrate

mode	R_{12} (Å)	θ_1 (deg)	ϕ_1 (deg)	θ_2 (deg)	ϕ_2 (deg)	DCO results V_{12}^a cm^{-1}	DCO results R^{+a} 10^{-44} esu^2 cm^2	DFT results V_{12} cm^{-1}	DFT results R^+ 10^{-44} esu^2 cm^2
Directions of the Transition Dipole Moment along the Chemical Bonds									
OH	2.95	90	87.3	8.6	251.0	−0.28	−171.2	0.85	−190.9
C=O	4.70	90	127.4	104.5	51.1	3.60	140.8	1.15	277.6
No Approximation for the Direction of the Transition Dipole Moment									
OH	2.95	90	89.5	39.0	268.5	−1.30	−134.7	0.85	−190.9
C=O	4.70	90	114.5	130.7	56.8	2.45	420.4	1.15	277.6

^{a} Calculated from eqs 4 and 5 using $\mu = 1.03 \times 10^{-19}$ esu cm and $\nu_0 = 3538$ cm^{-1} for the OH mode and $\mu = 2.34 \times 10^{-19}$ esu cm and $\nu_0 = 1753$ cm^{-1} for the C=O mode.

OH mode. This study clearly shows the limitations of the coupled oscillator model in interpreting the VCD in the OH stretching region. The splitting of the in-phase and out-of-phase modes does not seem to be correctly calculated. This feature is certainly due to the intramolecular hydrogen bonding between the OH and C=O groups that perturb the OH oscillator. Indeed, this perturbation is not taken into account in the calculation of the potential energy of interaction V_{12}.

4. Conclusions

This paper shows that the modeling of vibrational circular dichroism spectra using density functional theory can be successfully performed to determine the absolute configurations and conformations of chiral molecules. This methodology, which consists of the comparison of the experimental and calculated spectra of one enantiomer with a given conformation, was applied to dimethyl-L-tartrate in CCl₄ solution. The experimental absorption and VCD spectra were interpreted in terms of the trans COOR conformation with hydrogen bonding between the OH and C=O groups attached to the same chiral carbon. The calculated VCD spectrum reproduces very well the bisignate shapes (signs and intensities) observed for the OH, C=O, and C−O stretching vibrations. Finally, we have shown that the degenerate coupled-oscillator model can be used to interpret the Lorentzian derivative shape in the C=O stretching region, but it presents some limitations in the OH stretching region.

References and Notes

(1) Nafie, L. A.; Dukor, R. K.; Freedman, T. B. *Handbook of Vibrational Spectroscopy*; Chalmers, J. M., Griffiths, P. R., Eds; Wiley & Sons: Chichester, England, 2002; Vol 1, pp 731−744.

(2) Stephens, P. J.; Delvin, F. J. *Chirality* **2000**, *12*, 172.

(3) Holzwarth, G.; Chabay, I. *J. Chem. Phys.* **1972**, *57*, 1632.

(4) Tinoco, I. *Radiat. Res.* **1963**, *20*, 133.

(5) Keiderling, T. A.; Stephens, P. G. *J. Am. Chem. Soc.* **1977**, *99*, 8061.

(6) Su, C. N.; Keiderling, T. A. *J. Am. Chem. Soc.* **1980**, *102*, 511.

(7) Keiderling, T. A. *Appl. Spectrosc. Rev.* **1981**, *17*, 189.

(8) Freedman, T. B.; Balukjian, G. A.; Nafie, L. A. *J. Am. Chem. Soc.* **1985**, *107*, 6213.

(9) Polavarapu, P. L.; Ewig, C. S.; Chandramouly, T. *J. Am. Chem. Soc.* **1987**, *109*, 7382.

(10) Stephens, P. J.; Delvin, F. J.; Chabalowski, C. F.; Frisch, M. J. *J. Phys. Chem.* **1994**, *98*, 11623.

(11) Hehre, W. J.; Schleyer, P. R.; Radom, L.; Pople, J. A. *Ab Initio Molecular Orbital Theory*; Wiley: New York, 1986.

(12) Wong, M. W.; Frisch, M. J.; Wiberg, K. B. *J. Am. Chem. Soc.* **1991**, *113*, 4776.

(13) Frisch, M. J.; Trucks, G. W.; Schlegel, H. B.; Scuseria, G. E.; Robb, M. A.; Cheeseman, J. R.; Zakrzewski, V. G.; Montgomery, J. A., Jr.; Stratmann, R. E.; Burant, J. C.; Dapprich, S.; Millam, J. M.; Daniels, A. D.; Kudin, K. N.; Strain, M. C.; Farkas, O.; Tomasi, J.; Barone, V.; Cossi, M.; Cammi, R.; Mennucci, B.; Pomelli, C.; Adamo, C.; Clifford, S.; Ochterski, J.; Petersson, G. A.; Ayala, P. Y.; Cui, Q.; Morokuma, K.; Malick, D. K.; Rabuck, A. D.; Raghavachari, K.; Foresman, J. B.; Cioslowski, J.; Ortiz, J. V.; Stefanov, B. B.; Liu, G.; Liashenko, A.; Piskorz, P.; Komaromi, I.; Gomperts, R.; Martin, R. L.; Fox, D. J.; Keith, T.; Al-Laham, M. A.; Peng, C. Y.; Nanayakkara, A.; Gonzalez, C.; Challacombe, M.; Gill, P. M. W.; Johnson, B. G.; Chen, W.; Wong, M. W.; Andres, J. L.; Head-Gordon, M.; Replogle, E. S.; Pople, J. A. *Gaussian 98*; Gaussian, Inc.: Pittsburgh, PA, 1998.